International Journal of Control and Automation
Vol. 10, No. 10 (2017), pp.21-36
http//dx.doi.org/10.14257/ijca.2017.10.10.03

Networked Hierarchical Control Strategy for Voltage and Frequency in an Islanded Microgrid Considering Time Delay

Lizhen Wu[1, 2], Aihu Lei[1] and Xiaohong Hao[1]

[1]*College of Electrical and Information Engineering of Lanzhou University of Technology, Lanzhou, Gansu, 730050, China*
[2]*National Active Distribution Network Technology Research Center, Beijing Jiaotong University, Beijing, 100044, China*
[*]*Correspondence should be addressed to Aihu Lei, lahzhy@163.com*

Abstract

Due to the effect of line impedance and unequal load distribution, conventional droop control has limitations on the regulation of voltage, frequency and reactive power sharing in Microgrids (MGs) with multiple inverters paralleled. In this paper, a novel networked hierarchical control scheme based on networked control technology and hierarchical control theory is proposed. Also, a Distributed Secondary Controller (DSC) is designed using distributed consensus algorithm. Compared with the Centralized Secondary Control (CSC) approach by using a Microgrid Central Controller (MGCC), the DSC method not only can restore the frequency, voltage amplitude deviations produced by the local droop controllers and improve the accuracy of reactive power sharing, but also reduce the requirement of communication bandwidth, which makes the system more reliable and scalable. Finally, the simulation experiment platform is built based on Matlab/Simulink software. Real-time simulation results show the feasibility and good dynamic performance of the proposed method. Besides, the performance of the proposed control strategy is evaluated in regulating frequency and voltage of the MGs considering packet delays. The results indicate that the proposed algorithm is very robust with respect to packet delays. It provides a new approach for the application of networked control technology in microgrid system.

Keywords*: Microgrid; Droop control; Distributed consensus algorithm; Networked hierarchical control; Distributed secondary control; Packet delays*

1. Introduction

In recent years, in order to solve the access problem of distributed generations, coordinate the contradiction between large power grid and distributed generations and improve the comprehensive utilization of energy. The concept of Microgrids (MGs) has been proposed and attracted significant attention [1]. MG as a kind of special distributed generation system, which integrate a variety of renewable energy sources, energy storage, local load, monitoring protection device and the local power supply system of control units, which can autonomously operate in islanded mode or connected to the main grid [2].The distributed generators (DGs) in microgrid is mainly through the power electronic equipment access to the power distribution system. Voltage Source Inverters (VSIs) are usually used for all kinds of distributed generation interfaces in MGs. In the large scale microgrid, due to the capacity limitation of single converter, multiple inverters are usually required to be connected in parallel through the MG. The voltage, frequency regulation and power sharing of the islanded microgrid with multiple inverters are difficult problems. In order to avoid circulating currents among the converters, the droop-control method is often applied [3]. However, in multiple inverters paralleled MGs, there are no

ISSN: 2005-4297 IJCA

inertias, and the nature of the networks is mainly resistive. Mismatches in the inverters physical parameters and in the line impedances that connect to inverters to the PCC degrade the power sharing accuracy. It will generate circulating current. The inherent tradeoff of this method between frequency and amplitude regulation in front of power sharing accuracy cannot be avoided in islanded mode. As aforementioned, several methods have been proposed to improve the reactive power sharing by improving the droop control mechanism. These approaches have changed the characteristics of traditional droop control, and most of the schemes are more complex and difficult to be applied in engineering practice [4]. To cope with this problem, hierarchical control structure was firstly proposed in reference [5], which consists of three levels: primary control, secondary control and tertiary control layer, so that the microgrid can easily achieve standardization, which have become gradually concerned by the industry. Some authors proposed secondary and tertiary controllers. The main problem to be solved in such works was the frequency control of the system [6]. However, voltage stability issue was not considered. In [7], the deviations of voltage and frequency are reduced by secondary control strategy was proposed. But the communication algorithm was adopted cannot achieve accuracy of reactive power sharing. Moreover, this kind of centralized control method is adopted to realize secondary control in microgrid, it requires that the microgrid central controller (MGCC) need to exchange information with all DGs, which lead to higher communication bandwidth and if the MGCC is broken down, this will cause paralysis of entire system. Consequently, it reduced the system reliability. In [8], a decentralized coordinated control strategy has been proposed recently based on agent communication, but the scale of system is limited by the number of required data exchanges.

In this paper, a networked hierarchical control structure is proposed, including primary control layer and secondary control layer. In the secondary control layer, distributed secondary controller and primary controller are combined together and embedded in every DG, which as a node in the networked control system (NCS) and exchanges information between secondary controllers through the network. From the NCS perspective, distributed secondary control (DSC) requires that every DG obtains the global average of the parameters of interest, *i.e.*, frequency, voltage, and active and/or reactive power, in order to derive the local control signals. Consequently, distributed consensus algorithm is used to achieve global averages. Compared to centralized secondary control (CSC), distributed secondary control can achieve data transmission and control independently, quickly and efficiently, and thus more suitable for practical application.

This paper is organized as follows. In Section II, the structure of networked hierarchical control and distributed consensus algorithm are described. Then, details of primary controller and distributed secondary controllers for MGs are discussed in Section III. Section IV provides simulation results of an islanded MG with four DGs. Conclusions are given in Section V.

2. Networked Hierarchical Control Approach for Islanded MicroGrids

2.1. Networked Hierarchical Control Structure Based on Consensus Algorithm

The conventional centralized control scheme may encounter severe challenges in applying a Networked Control System (NCS). Firstly, in order to achieve the optimal operating conditions, the MGCC will be required to have a high level of connectivity, which will impose a substantial computational burden and is more sensitive to failures and modeling errors than distributed control schemes. Another challenge is that the topology of the MGs is unknown, not only because of the variety of configurations of the power grid and communication network topologies, but also because “plug-and-play” technologies will make the topology time-varying. Thus, in order to control this kind of

NCS, a robust algorithm should be able to operate correctly in the presence of limited and unreliable communication capabilities, and often in the absence of a central control mechanism.

In order to achieve fully distributed control, this paper applies a dynamic consensus algorithm based networked hierarchical control method to realize accurate power sharing and voltage/frequency restoration. The consensus algorithm based networked hierarchical control scheme for an islanded MG is shown in Figure 1. In this architecture, primary and secondary controls are implemented in each DG unit. The secondary control is placed between the communication system and the primary control. In other word, the secondary control is locally embedded in each DG unit, as a smart node in the NCS; however, the local secondary control requires an underlying communication network to operate properly. Since the secondary control should collect the required data from all other units and produce appropriate control signal for the primary control using an averaging method. A scalable and robust approach is to employ distributed consensus algorithms, where a series of local exchanges among neighboring units ultimately yields the same global average at every DG. In turn, the local secondary controllers operate on these parameters, proposed communication algorithm is able to not only control frequency and voltage but also share power between units in the MG. Data exchange for DSC can be implemented in CAN bus.

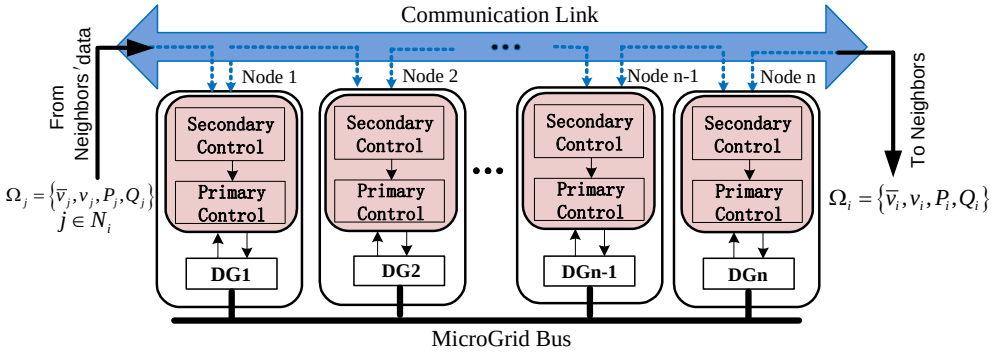

Figure 1. Proposed Networked Hierarchical Control Architecture for Islanded MGs

The topology of networked communication system is shown in Figure 2.For example, consider a four bus system where each bus has its own generator and load. Figure 2(a) shows the system communication topology when using the conventional central control. The center controller acquires all the information (loads, DG output powers, *etc.*) and calculates the deviation for each DGs. Due to all DG nodes exchange information with the central management node MGCC, so that the communication burden is very heavy, and if a control node is a failure can result in a bad function of the whole system. Even more unfortunately, if the MGCC node is failure, the whole system would be broken down. Obviously, the reliability of the conventional centralized control system is very poor. Figure 2(b) shows a networked control system with distributed control by using consensus algorithm. The nodes represent DGs and edges represent communication links for data exchange. The communication graph does not need to have the same topology as the underlying physical microgrid. In the NCS, the secondary controller (embedded in each DG unit) will update its own information based on its neighbors' information. According to the literature [9], the control system use the distributed consensus algorithm, even if one of the nodes is broken down, the system can achieve consensus convergence, which does not affect the stable operation of other nodes. Compared to the centralized network topology, the distributed network topology not only can reduce the communication

burden obviously, but also only require the lower communication bandwidth. Therefore, the distributed network topology is applied in this paper as shown in Figure 2(b).

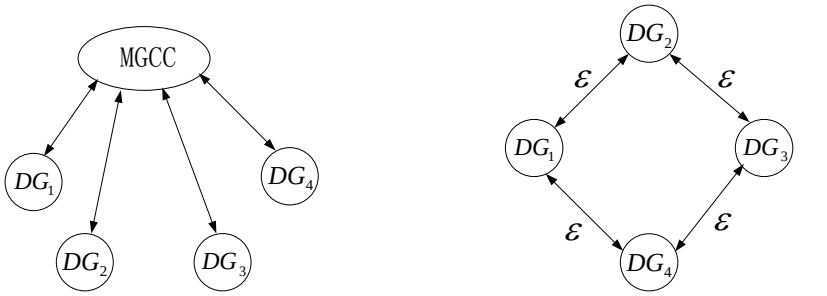

(a) Centralized Network Topology (b) Distributed Network Topology

Figure 2. Two Kinds of Network Topology Architecture

2.2. Distributed Consensus Algorithm

Consensus problems and algorithms find their roots in the computer science area [10]. In recent years, they have been more and more applied in multi-agent systems, coordinated control, congested control, crowd control, complex dynamical network, *etc.* The purpose of consensus algorithm is to allow a set of distributed agents to reach an agreement on a quantity of interest by exchanging information through communication network. In the MG systems, these algorithms can be used to achieve the information sharing and coordination control among distributed units. In order to analysis the proposed control approach of the next section conveniently, this section gives a brief introduction to the algorithm.

The basic consensus algorithm with continuous-time and discrete-time integrator agents can be described as [11],

$$\dot{x}_i(t) = -\sum_{j \in N_i} a_{ij}(x_i(t) - x_j(t)), \qquad i = 1,2,\cdots,n \tag{1}$$

Where x_i is the state of agent node i. The state variable x_i can be expressed as the physical quantity of the actual system, such as voltage, current, frequency, *etc.* a_{ij} indicates the connection status between node i and node j, if the nodes i and j are not neighboring nodes, then $a_{ij} = 0$. N_i is the set of indexes of the agents that are connected with agent i.

From a system point of view, the vector form of the iteration algorithm of the equation (1) can be expressed as

$$\dot{X} = -L_n X \tag{2}$$

Where L_n is the laplace matrix of network and related with the networked topology. Considering the discrete nature of communication data transmission, the discrete-time form of the consensus algorithm (1) is used in this paper as follows [12],

$$x_i(k+1) = \sum_{j=1}^{n} w_{ij}(k) x_i(k) = x_i(k) + \sum_{j \neq i} w_{ij}(k)(x_j(k) - x_i(k)), \qquad i = 1,2,\cdots,n \tag{3}$$

The vector form of equation (3) can be described as

$$X(k+1) = W(k)X(k) \tag{4}$$

Where $W(k) \in R^{n \times n}$ is the weight matrix of the communication network. The weight matrix is designed to a kind of random matrix and the elements of row or column of the matrix adds up to 1, the largest eigenvalue is single 1, the module of the rest of eigenvalues are less than 1. If the $W(k)$ is designed to double random symmetric matrix, then the final consensus equilibrium value will be achieved and presented as

$$\overline{x}_i(k) = \frac{1}{n}\sum_{j=1}^{n} x_i(0), \qquad i = 1, 2, \cdots, n \tag{5}$$

The detailed proof of the algorithm convergence can be found in [12]. In this paper, the initial values are the locally measured DG terminal voltage and the inductor current.

The communication delays of the actual networked control system is inevitable, the distributed consensus algorithm with time delays can be expressed as [13]

$$U_i(k+1) = \sum_{j=1, j\neq i}^{n} w_{ij} U_j(k-\tau) + w_{ij} U_i(k) \tag{6}$$

$$L_i^*(k) = \sum_{j=1, j\neq i}^{n} w_{ij} L_j(k-\tau) + w_{ij} U_i(k) \tag{7}$$

Where τ is the communication delay, which is the integral multiple of sampling period T_s .When τ is less than T_s , the communication delays have no effect on consensus convergence and when τ is larger, the characteristic of consensus convergence is determined by the matrix $W(k)$.

The designing method of dynamic matrix ($W(k)$) is very important, for the sake of guarantee the system convergence and have a good robustness with consideration of communication delays. In [10], if the $W(k)$ is designed to non-negative double random symmetric matrix and the diagonal elements are not zero, thus the convex hull of point $U_i(k)$ will reduce or maintain a constant value, the communication delays have little effect on consensus convergence.

In summary, distributed consensus algorithm can be adopted in the distributed secondary control, not only can reduce the effect of time delays on the system robustness, but also avoid the situation that centralized control relies on MGCC excessively .Thus, it improves the reliability and flexibility of microgrid. The details of primary controller and distributed secondary controller are introduced elaborately in the next section.

3. Voltage and Frequency Control Based on DSC

Figure 3 depicts the details of networked hierarchical control for an individual DG unit (DG_i) in an islanded MG. It can be seen that the power stage of each DG consists of a DC power, an interface inverter and an LC filter. Note that, the other DGs have the same power stage, but the line impedances are different. The local controller of each DG consists of voltage and current control loops, virtual impedance loop, and traditional active/reactive power droop control loop, which generate the gate signals for DGs interface inverters. The secondary controller generates the unbalance compensation of PCC voltage in microgrid by sending proper control signals to the DGs local controllers. Discrete distributed consensus algorithm is applied in the distributed secondary control level, which the global average values are obtained. Each converter transmits a set of data, $\Omega_j = \{\overline{v}_j, v_j, P_j, Q_j\}$ to its neighbors. The dataset transmitted by node i , Ω_j consists of four elements; its estimate of the average voltage across the microgrid $\overline{v}_j$, the measured local voltage v_j , and the measured per-unit active/reactive power P_j, Q_j . At the other end of the communication links, each converter j receives data from all its neighbors Ω_k ,

$k \in N_j$ with communication weights a_{jk} .These communication weights are design parameters and can be considered as data transfer gains.

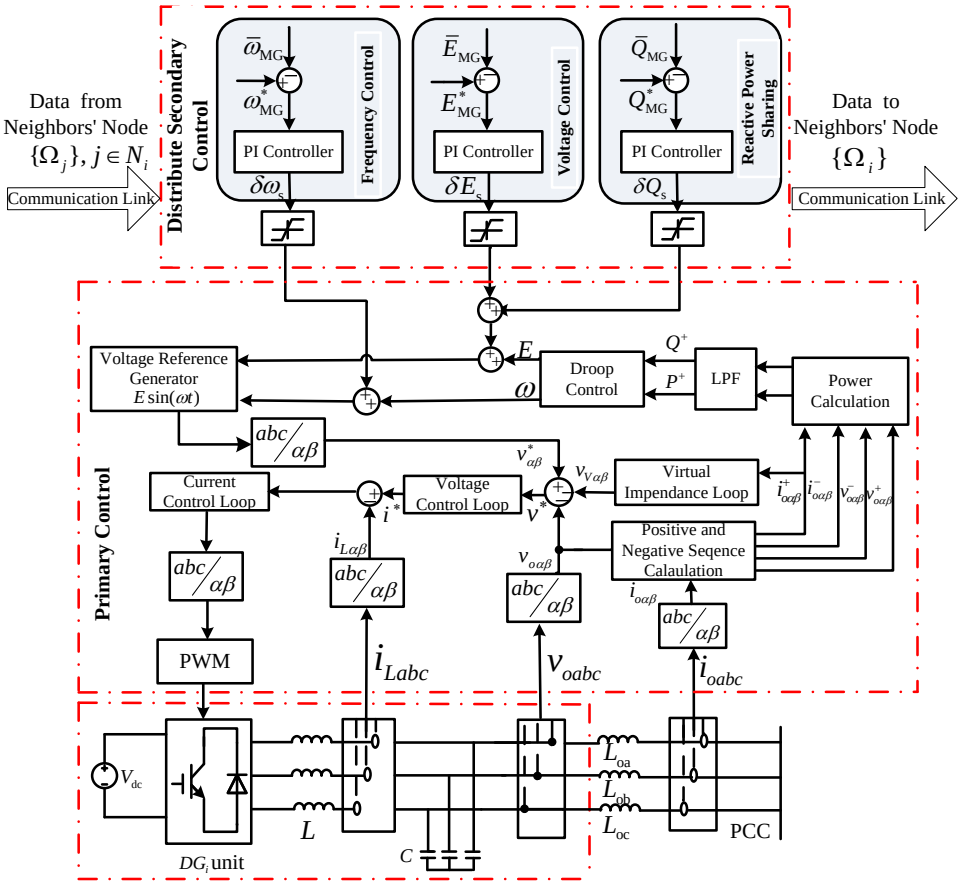

Figure 3. Structure of Distributed Secondary Control for a DG Unit in Islanded Microgrids

The global voltage/frequency regulation and proportional reactive power sharing are the two objectives of the secondary/primary control, which require proper voltage set point assignment for the individual inverters. The proposed secondary controller is highlighted in Figure 3, where local and neighbors' information are processed to adjust the local voltage/frequency set point. The starting point is the conventional droop mechanism that characterizes the converter output impedance using virtual impedance. The droop controller, at a primary control level, acts on local information. When operating conditions vary, the droop mechanism promptly initiates the voltage/frequency adjustment. However, this local control has a limited performance. Cooperation among inverters, at the secondary control level, the global average values can help properly fine-tune the voltage set points.

3.1. Design of Primary Controller

In Figure 3, the two-phase stationary $\alpha\beta$ reference frame of primary controller is adopted in this paper. Power calculation is done according to the instantaneous reactive power theory [14]. As explained in [14], the instantaneous values of three-phase active and reactive powers can be calculated according to the following equations, respectively:

$$\begin{cases} p = v_{o\alpha} i_{o\alpha} + v_{o\beta} i_{o\beta} \\ q = v_{o\beta} i_{o\alpha} - v_{o\alpha} i_{o\beta} \end{cases} \tag{8}$$

Where $v_{o\alpha}$ and $v_{o\beta}$ are capacitor voltages in $\alpha\beta$ reference frame; $i_{o\alpha}$ and $i_{o\beta}$ are fundamental currents. Each of the instantaneous powers calculated using equation (8) consists of dc and ac (oscillatory) components. The dc components are fundamental positive-sequence (FPS) active and reactive powers that can be extracted using low-pass filters (LPFs) [14].Thus, the FPS active and reactive powers (P^+ and Q^+, respectively) can be controlled by the angular frequency and amplitude of the DG unit FPS output voltage, respectively. According to this condition, the following droop characteristics are considered for the sharing of FPS power among the DGs of an islanded microgrid:

$$\begin{cases} \omega^* = \omega_0 - (k_p + k_d s) P^+ \\ E^* = E_0 - k_q Q^+ \end{cases} \tag{9}$$

Where S is Laplace variable; ω^* and E^* are angular frequency reference and voltage amplitude reference, respectively. ω_0 and E_0 are rated angular frequency and rated voltage amplitude, respectively. k_p is active power proportional coefficient, k_q is reactive power proportional coefficient. In order to increase the response speed and help to improve the dynamic behavior of the power control [15], the differential term k_d is applied to the droop control.

In the low-voltage microgrid system, the line impedances between power sources are resistive. The accuracy of reactive power sharing provided by droop controllers is affected by output impedance of the DG units and line impedances. Therefore, the virtual inductance is considered to make the DG output impedance more inductive to improve the decoupling of P^+ and Q^+ . Furthermore, the virtual output impedance can provide additional features such as the hot-swap operation and sharing of nonlinear load [16], [17]. The virtual impedance is implemented can be expressed as

$$\begin{cases} v_{V\alpha} = R_{\mathrm{v}} i_{o\alpha}^+ - L_{\mathrm{v}} \omega^* i_{o\beta}^+ \\ v_{V\beta} = R_{\mathrm{v}} i_{o\beta}^+ + L_{\mathrm{v}} \omega^* i_{o\alpha}^+ \end{cases} \tag{10}$$

Where R_{v} and L_{v} are the virtual resistance and inductance values, respectively. $i_{o\alpha}^+$ and $i_{o\beta}^+$ are the FPS components of current in the $\alpha\beta$ frame, $v_{V\alpha\beta} = [v_{V\alpha}, v_{V\beta}]$ is the virtual impedance output voltage.

Due to the difficulties of using proportional-integral (PI) controllers to track non-dc variables, proportional-resonant (PR) controllers are usually preferred to control the voltage and current in the $\alpha\beta$ stationary reference frame. In this paper, the following PR voltage and current controllers can be presented as [18]

$$\begin{cases} G_V(s) = k_{pV} + \dfrac{2k_{rV} \cdot \omega_{\mathrm{cV}} \cdot s}{s^2 + 2\omega_{\mathrm{cV}} \cdot s + \omega_0^2} \\ G_I(s) = k_{pI} + \dfrac{2k_{rI} \cdot \omega_{\mathrm{cI}} \cdot s}{s^2 + 2\omega_{\mathrm{cI}} \cdot s + \omega_0^2} \end{cases} \tag{11}$$

Where k_{pV} (k_{pI}) and k_{rV} (k_{rI}) are the proportional and resonant coefficients of the voltage (current) controller, respectively. Also, ω_{cV} and ω_{cI} represent the voltage and current controller cut-off frequencies, respectively. ω_0 is the resonant angular frequency.

3.2. Design of Secondary Controllers Based on Distributed Consensus Algorithm

Using the consensus algorithm as the basic framework, the conventionally centralized control problem can be solved in a distributed manner. In this section, we illustrate the use of the distributed consensus algorithm. In order to restore the deviations of voltage and frequency generated by the primary control, improve the accuracy of reactive power sharing, a distributed secondary controller is designed based on distributed consensus algorithm.

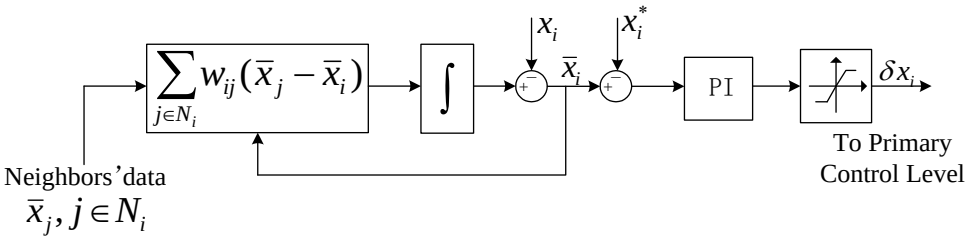

Figure 4. State Observer and Compensation Value

In the secondary control, a state observer is constructed with the distributed consensus algorithm [13] [19], which are used to obtain global average value. Figure 4 shows the cooperative distributed approach for the global averaging. The observer at node i receives its neighbors' estimates $\bar{x}_j$ ($j \in N_i$). Then, the observer updates its own estimate $\bar{x}_i$ by processing the neighbors' estimates and the local state measurement x_i. Using the four DGs as an example, the data sets Ω_j are achieved from neighborhood j, according to the distributed consensus algorithm as shown in equations(3)~(5), if the $W(k)$ is double random matrix, for arbitrary $i \in [0, N]$, N is the sum of DG units, then data sets $\bar{\Omega}_i$ will converge to a global average can be expressed as

$$\lim_{k\to\infty} \bar{\Omega}_i(k) = \frac{1}{N}\sum_{i=1}^{N} \Omega_i(k) \tag{12}$$

Then calculate the difference between expected value and average value of the output voltage of every DG_i, meanwhile the difference will be transmitted to PI controller and amplitude limiting implement, ultimately achieve the compensation values δx_i .where x_i is the amplitude of DG_i output, $\bar{x}_j$ and $\bar{x}_i$ are the average value of the corresponding quantities obtained from node j and node i, respectively. x_i^* is the expected value of DG_i output.

In order to guarantee the convergence characteristic of system and have a good robustness with consideration of communication delays, the $W(k)$ matrix can be designed according to the Metropolis constructed method that proposed in the literature [20] and can be presented as

$$w_{ij}=\begin{cases}\dfrac{1}{\max(n_i,n_j)+1}, & j\in N_i\\ 1-\sum_{j\in N_i} w_{ij}, & i=j\\ 0, & others\end{cases} \tag{13}$$

Where $\max(n_i,n_j)$ represents this node and its neighboring nodes have a larger number of neighbors. According to the above method, the double random matrix $W(k)$ can be expressed as

$$W(k)=\begin{bmatrix}1/3 & 1/3 & 0 & 1/3\\ 1/3 & 1/3 & 1/3 & 0\\ 0 & 1/3 & 1/3 & 1/3\\ 1/3 & 0 & 1/3 & 1/3\end{bmatrix} \tag{14}$$

In Figure 3, secondary control in each DG collects all the measured value (frequency, voltage amplitude and reactive power) of other DG units by using the communication system and produces appropriate control signals that send to the primary control layer to remove the steady-state errors. Therefore, the average values of angular frequency, voltage amplitude and the reactive power of DG units can obtain as follows.

$$\begin{cases}\bar{\omega}_{MG}=\dfrac{1}{N}\sum_{i=1}^{N}\omega_{DGi}\\ \bar{E}_{MG}=\dfrac{1}{N}\sum_{i=1}^{N}E_{DGi}\\ \bar{Q}_{MG}=\dfrac{1}{N}\sum_{i=1}^{N}Q_{DGi}\end{cases} \tag{15}$$

The average values are compared with the nominal angular frequency ω_{MG}^{*}, voltage E_{MG}^{*} and reactive power Q_{MG}^{*} of MG and sent the difference to the primary controller of DG_i to correct the angular frequency, voltage and reactive power as follows:

$$\begin{cases}\delta\omega_s=k_{pf}(\omega_{MG}^{*}-\bar{\omega}_{MG})+k_{if}\int(\omega_{MG}^{*}-\bar{\omega}_{MG})dt\\ \delta E_s=k_{pE}(E_{MG}^{*}-\bar{E}_{MG})+k_{iE}\int(E_{MG}^{*}-\bar{E}_{MG})dt\\ \delta Q_s=k_{pQ}(Q_{MG}^{*}-\bar{Q}_{MG})+k_{iQ}\int(Q_{MG}^{*}-\bar{Q}_{MG})dt\end{cases} \tag{16}$$

Where k_{pf}, k_{pE} and k_{pQ} are the proportional coefficients of PI controller, respectively. k_{if}, k_{iE} and k_{iQ} are the integral coefficients of PI controller, respectively. $\bar{\omega}_{MG}$ is the average angular frequency, $\bar{E}_{MG}$ is the average voltage and $\bar{Q}_{MG}$ is the average reactive power. $\delta\omega_s$, δE_s and δQ_s are compensation values sent to the primary control level in order to restore the deviations, respectively.

Therefore, the input ω_i and E_i of the three-phase voltage reference generating module are obtained, the calculating equation of ω_i and E_i can be expressed as

$$\begin{cases} \omega_i = \omega^* + \delta\omega_s \\ E_i = E^* + \delta E_s + \delta Q_s \end{cases} \tag{17}$$

4. Simulation Experiment Results Analysis

In order to evaluate the effectiveness of the proposed control strategy, a simulation experiment platform of an islanded microgrid is built based on Matlab/Simulink software, as shown in Figure 5, which includes four DGs. All DG units in the system have the same power rate of 3kW, and each one is supporting a local load. The line impedance between DG_1 and DG_3 to PCC can be presented as $Z_1 = Z_3 = 0.16 + j0.105$, DG_2 and DG_4 to PCC can be presented as $Z_2 = Z_4 = 0.32 + j0.21$.That the ratio of them is 2:1. Switching frequency of the DGs inverters is set to 10 kHz. The simulation parameters of the power stage and control system are shown in Table1.

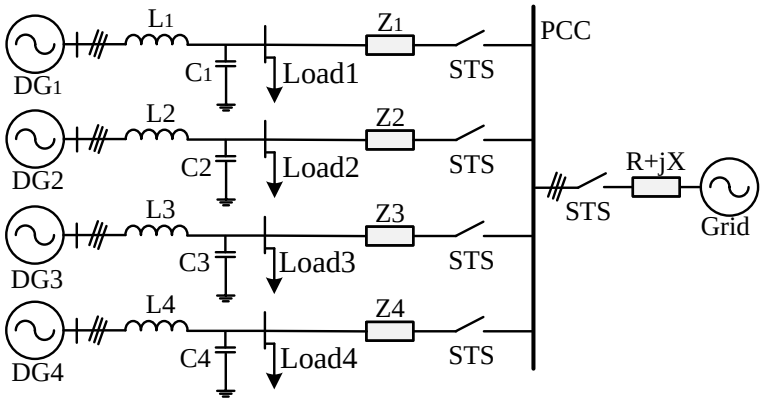

Figure 5. Structure of Simulation-Testing System

Table 1. Power Stage and Control System Parameters

Parameter	Symbol	Value	Parameter	Symbol	Value
Rated Voltage	E	311V	Frequency Proportional term	k_{pf}	0.01
Rated Frequency	f	50Hz	Frequency Integral term	k_{if}	$4s^{-1}$
DC Voltage	V_{dc}	650V	Voltage Proportional term	k_{pE}	0.01
Resistive Load	R_L	200/400Ω	Voltage Integral term	k_{iE}	$0.6s^{-1}$
Output Inductance	L_0	1.8mH	Reactive Power Proportional term	k_{pQ}	0.00001Var/V
Filter Inductance	L	1.8mH	Reactive Power Integral term	k_{iQ}	0.3Var/Vs
Filter Capacitance	C	25μF	PLL time constant	τ	0.05s
Active Power droop term	k_p	0.008Ws/rd	Active Power differential term	k_d	0.00002
Reactive Power droop term	k_q	0.16Var/V	dSPACE Sampling Frequency	f_s	10kHz

4.1. Dynamic Performance Analysis of Distributed Secondary Control System

For the sake of simplicity, when analyzes the system dynamic performance of distributed secondary control, the communication delay was assumed to be negligible.

Firstly, during the first 5s of operation, the voltage amplitude and frequency are controlled by the primary droop controller, so that the output power sharing of the DGs is completed. The simulation results are shown in Figure 6. From Figure 6(a) and (b), it can be observed that the steady-state frequency and voltage deviations of DGs exist, and the accuracy of reactive power sharing is affected by the line impedance and the sharing deviation is also existed as shown in Figure 6(d). In order to remove the deviations, the proposed DSC is implemented at t=5s, and as can be seen, the system frequency and voltage are regulated successfully and the deviations are eliminated at about t=10s, basically reach the rated value. Besides, reactive power is properly shared between DGs.

In order to test the dynamic performance of DSC, where a 200-Ω pure resistive load is connected for a short time at t=20s and then disconnected at t=30s. As can be observed from Figure 6(a) and (b), DSC can eliminate the voltage and frequency fluctuating deviations quickly that caused by rapid load variations. Figure 6(c) depicts the corresponding active power injections of four units in the same conditions, illustrating that the primary P-f droop control approach is effective to share the active power accurately between DG units.

Based on the analysis above, it can be seen that the primary droop control alone is not able to equalize the reactive power of DGs in the MG. After implementing the DSC, reactive power is properly shared between DGs, even in the presence of load variations. Also it illustrates that the DSC also has a good performance.

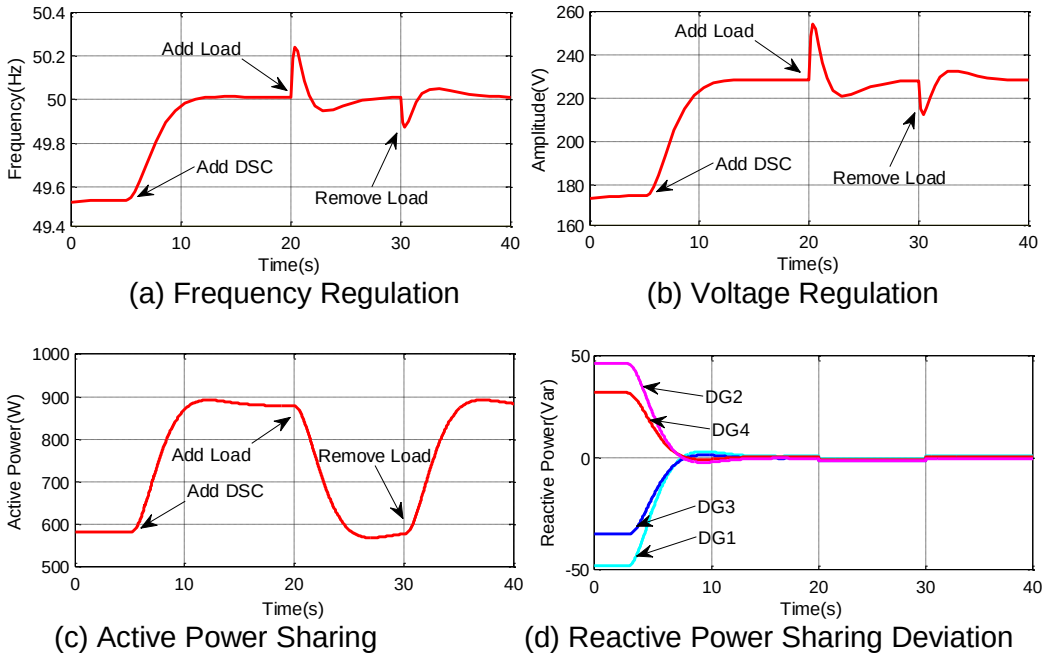

(a) Frequency Regulation (b) Voltage Regulation

(c) Active Power Sharing (d) Reactive Power Sharing Deviation

Figure 6. Dynamic Performance Evaluation of Microgrid Based on Distributed Secondary Control

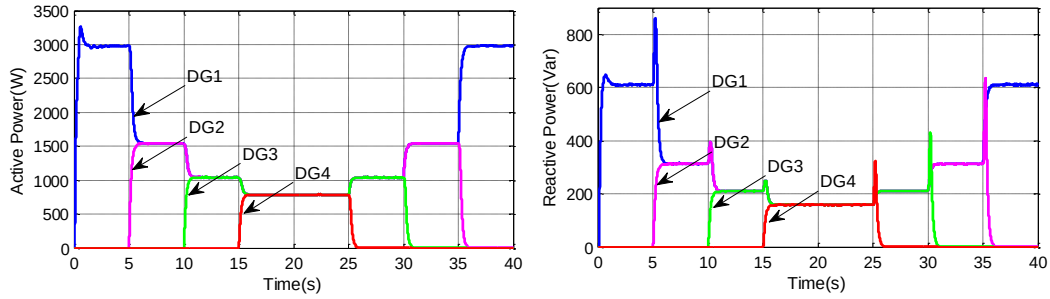

(a) Active Power with DG Excluding/ Including

(b) Reactive Power with DG Excluding/ Including

Figure 7. Plug-and-Play Verification

In addition, the Plug-and-play capacity can be verification from Figure 7. Firstly, at start period (t=0s), the active power load (3kW) and reactive power load (600Var) are connected to the microgrid. Afterword, the four DGs are connected sequentially to the microgrid (at t=0s, 5s, 10s, 15s respectively), during 5s of operation, the four DGs are disconnected at t=20s, 25s, 30s, 35s respectively. The simulation results are shown in Figure 7(a) and (b). As can be seen, in the process of DG adding and removing, the system can run stably and output active and reactive power can be shared accurately. From this we can obtain that the system can achieve the plug-and-play function.

4.2. Analysis of System Stability Considering Time Delay

With development of network control system theory and applications, the influence of network delay to network control system should be considered. It is one of the most important factors of worsening system performance, delaying information not to arrive on time and arousing system unstable. Specifically, the effects of three different delays on the performance of the control system are studied. In order to simulate the low bandwidth communication characteristics of the secondary control layer and primary control layer, adding a delay module between the compensation signals of secondary control layer to the primary control layer, the delay module is directly connected to the PI controller of the secondary control. Taking the frequency secondary control as an example, the control structure is shown in Figure 8.

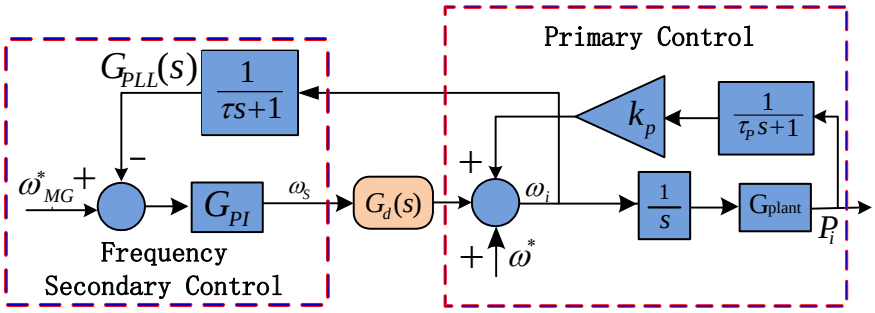

Figure 8. Structure of Distributed Secondary Control Considering Time Delay

The transfer function of the delay module can be presented as

$$G_d(s) = \frac{1}{T_d s + 1} \tag{18}$$

Where T_d is the network communication delay of each block. It can be simulate the communication time delay of secondary control by setting different value. For the sake of simplicity, here only voltage and frequency responses are represented.

In order to illustrate the superiority of the proposed distributed secondary control (DSC), comparing with the performance of central secondary control (CSC) for three amounts of fixed communication delay, 0.2s, 1s and 2s. Figure 9 depicts the effects of the communication delay on the control strategies performance, when they remove voltage and frequency deviations. Firstly, a 200-Ω pure resistive load is connected at t=20s and then disconnected at t=30 s. As can be seen, when the DSC tries to eliminate voltage and frequency deviations caused by frequent load changing, the communication delay will affect the system output. From Figure 9(a) and (b), it can be observed that both DSC and CSC can adjust frequency and voltage deviations caused by load variations for the time delay of 0.2s and have a good performance, but the response speed of DSC is more faster. When the time delay is less than 1s, the system responses of two control methods are all acceptable. However, compared to the control effect of CSC, DSC has a better control performance in frequency and voltage recovery, and the overshoot is small, which shows the system has a good robustness as can be observed in Figure 9(c) and (d). From Figure 9(e) and (f), even if the time delay is 2s, the DSC slowly but successfully regulates voltage and frequency deviations caused by load variations, but CSC has a big fluctuation and the adjusting time of system is very long.

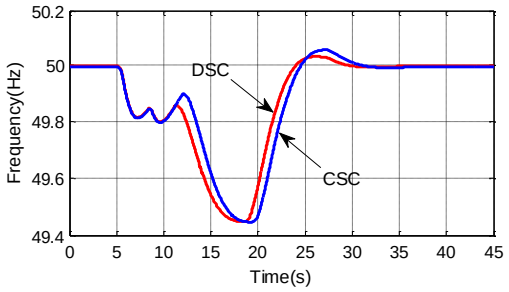

(a) 0.2s Time Delay

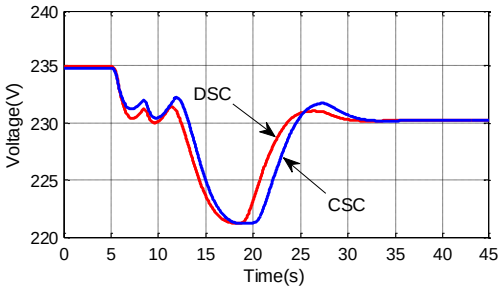

(b) 0.2s Time Delay

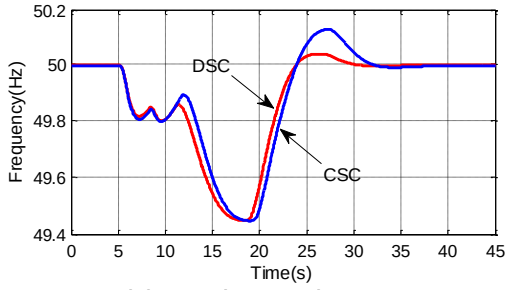

(c) 1s Time Delay

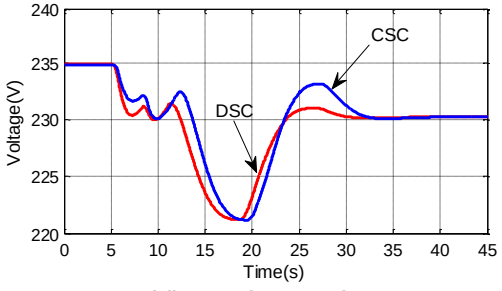

(d) 1s Time Delay

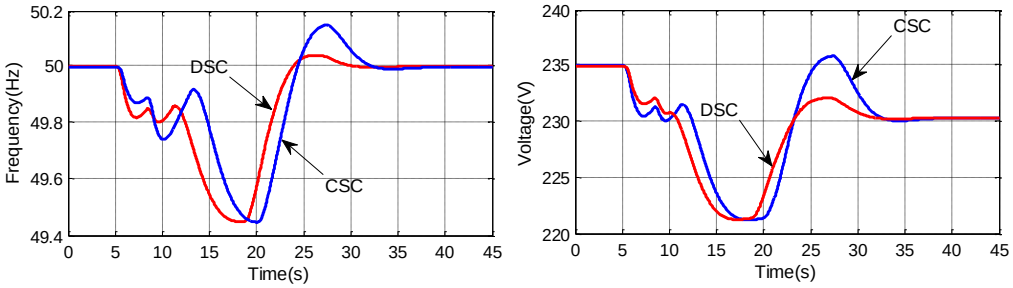

(e) 2s Time Delay (f) 2s Time Delay

Figure 9. Dynamic Performance Evaluation of DSC Considering Packet Delay

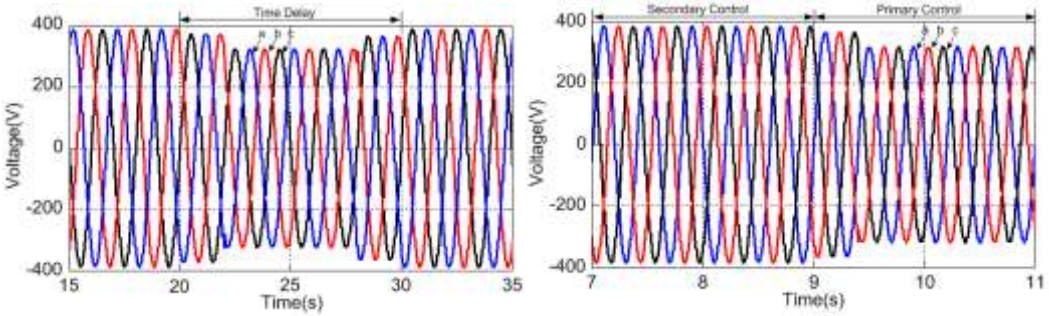

(a) 5s Time Delay (b) 10s Time Delay

Figure 10. DG Output Three-phase Voltage in the Case of Longer Time Delay

In order to further illustrate the effect of longer time delay on the output voltage of microgrid, analyses the DG output three-phase voltage in case of 5s and 10s time delays circumstances, the simulation results are shown in Figure 10. As can be seen from Figure 10(a), because of the existence of a longer delay (such as 5s), DG output three-phase voltage produces a large deviation over a period of time, after a slow adjustment, the DG output three-phase voltage gradually recovers to the rated value. As can be observed from Figure 10(b), due to the existence of a very long delay (such as 10s), system loses the secondary control to adjust the deviation, only exists primary control. So there is a enormous deviation between DG output three-phase voltage, thus the system is unstable. Besides, for the packet loss, it can be processed in accordance with long time delay.

5. Conclusions

In this paper, the problems of voltage, frequency stability control and reactive power sharing of microgrid are studied. It proposes a networked hierarchical control strategy. Distributed consensus algorithm is applied to design distributed secondary controller that eliminates the voltage, frequency and reactive power sharing deviations. The system dynamic performance is researched by a microgrid simulation platform with four DG units in parallel. Simulation results show the proposed distributed secondary control method can control the system frequency and voltage preferably, even if in the low X/R circumstances, the reactive power sharing is also very accurate. Besides, it also validates that the proposed approach can achieve the plug-and-play function. Compared to the centralized secondary control, distributed secondary control method has a good dynamic performance and robustness, which is adopted in the networked hierarchical control. Meanwhile, the dynamic performance of control system is also studied in the presence of communication delays and data packet losses. The simulation results show the system

stability is not affected by the short communication time delay, however, the system will be unstable in the case of long communication delay. The results confirm the validity and feasibility of the proposed control method. This paper provides theoretical basis for the microgrid system using networked control method.

Acknowledgments

This work was supported by the National Natural Science Foundation of China (No.51467009), the Science and Technology Foundation of STATE GRID Corporation of China, the project of Lanzhou science and technology plan (No.2016-3-67).

References

[1] A. Claudio, Cañizares and R.P. Behnke, " Trends in Microgrid Control. IEEE Transactions on Smart Grid", vol. 5, no. 4, **(2014)**, pp. 1905-1918.
[2] J.M. Guerrero, J.E Vasquez, Matas and J. de Vicuna, "Hierarchical Control of Droop-Controlled AC and DC Microgrids-A General Approach Toward Standardization", IEEE Transactions on industrial Electronics, vol. 58, no. 1, **(2011)**, pp. 158-172.
[3] Y.A.R.I. Mohamed and A.A. Radwan, "Hierarchical control system for robust microgrid operation and seamless mode transfer in active distribution systems," IEEE Trans. Smart Grid, vol. 2, no. 2, **(2011)**, pp. 352-362.
[4] J. Peng, A. Xin and W. Yonggang, "Reactive power control strategy of microgrid using potential function method", Proceedings of the CSEE, vol. 32, no. 25, **(2012)**, pp. 44-51(in Chinese).
[5] J.M. Guerrero, M. Chandorkar, Matas, T. Lee and P.C. Loh, "Advanced Control Architectures for Intelligent Microgrids-Part I: Decentralized and Hierarchical Control", IEEE Transactions on industrial Electronics, vol. 60, no. 4, **(2013)**, pp. 1254-1262.
[6] M. Yiwei, Y. Ping, C. Sizhe, Z. Zhuoli and W. Yuewu, "Frequency hierarchical control for islanded microgrid consisting of diesel generator and battery energy storage system", Control Theory and Applications, vol. 32, no. 8, **(2015)**, pp. 1098-110.(in Chinese)
[7] J. Vasquez, J. M. Guerrero, M. Savaghebi, J.E. Garcia and R. Teodorescu, "Modeling, analysis, and design of stationary reference frame droop controlled parallel three-phase voltage source inverters", IEEE Transactions on industrial Electronics, vol. 60, no. 4, **(2013)**, pp. 1271-1280.
[8] A. Bidram, A. Davoudi and Z. Qu, "Secondary control of microgrids based on distributed cooperative control of multi-agent systems", IET Gener. Transm. Distrib, vol. 7, no. 8, **(2013)**, pp. 822-831.
[9] Z.A. Zhang, M.Y. Chow, "Convergence analysis of the incremental cost consensus algorithm under different communication network topologies in a smart grid", IEEE Transactions on Power Systems, vol. 27, no. 4, **(2012)**, pp. 1761-1768.
[10] L. Hui, F. Xiaoping and L. Shaoqiang, "Review of distributed consensus problem in multi-agent system", Computer Engineering and Applications, vol. 49, no. 1, **(2013)**, pp. 36-42. (in Chinese).
[11] Z.A. Zhang, X.Z. Ying and M.Y. Chow, "Decentralizing the economic dispatch problem using a two-level incremental cost consensus algorithm in a smart grid environment", 2011 North American Power Symposium. Boston, MA: IEEE, **(2011)**, pp. 1-7.
[12] X. Ying, M. Y. Chow, "Sampling rate selection influences on incremental cost consensus algorithm in decentralized economic dispatch", 38th Annual Conference on Industrial Electronics Society, **(2012)**, pp. 1410-1415.
[13] Z. Lv, Z. Wu, X. Dou and M. Hu, "A Distributed Droop Control Scheme for Islanded DC Microgrid Considering Operation Costs", Proceedings of the CSEE, vol. 36, no. 4, **(2016)**, pp. 900-910(in Chinese).
[14] A. Ovalle, G. Ramos, S. Bacha and A. Hably, "Decentralized Control of Voltage Source Converters in Microgrids Based on the Application of Instantaneous Power Theory", IEEE Transactions on Industrial Electronics, vol. 62, no. 2, **(2015)**, pp. 1152-1162.
[15] E. Pouresmaeil, M. Mehrasa and J. P. S. Catalão, "A Multifunction Control Strategy for the Stable Operation of DG Units in Smart Grids", IEEE Transactions on Smart Grid, vol. 6, no. 2, **(2015)**, pp. 598-607.
[16] L. Wu, X. Yang and X. Hao, "Networked hierarchical control scheme for voltage unbalance compensation in an islanded microgrid with multiple inverters", International Journal of Innovative Computing, Information and Control, vol. 11, no. 6, **(2015)**, pp. 2089-2102.
[17] J. He and Y. W. Li, "Analysis and design of interfacing inverter output virtual impedance in a low-voltage microgrid", in Proc. ECCE, **(2010)**, pp. 2857-2864.
[18] J. He and Y. Li, "An Enhanced Microgrid Load Demand Sharing Strategy", IEEE Transactions on Power Electronics, vol. 27, no. 9, **(2012)**, pp. 3984-3995.
[19] L Meng, X Zhao, F Tang and M Savaghebi, "Distributed Voltage Unbalance Compensation in Islanded Microgrids by Using a Dynamic Consensus Algorithm", IEEE Transactions on Power Electronics, vol. 31, no. 1, **(2016)**, pp. 827-838.

[20] P. Li, Y. Lu, X. Bai and H. Wei, "Decentralized optimization for dynamic economic dispatch based on alternating direction method of multipliers", Proceedings of the CSEE, vol. 35, no. 10, **(2015)**, pp. 2428-2435. (in Chinese).

Authors

Wu Lizhen, she received the M.S. degree in the control theory and control engineering from Lanzhou University of Technology, Gansu, China, in 2004.And now she is studying for her doctorate in power system & its automation in National Active Distribution Network Technology Research Center. Currently, she is an Associate Professor/Master Supervisor at College of Electrical and Information Engineering Lanzhou University of Technology, where she teaches courses on power electronics, control theory and renewable energy systems. Her interests include Photovoltaic, wind energy conversion, storage energy systems, and microgrids; power system control and distribute generation sources connected to the distribution network, networked control theory and its application.

Lei Aihu, he was born in Lanzhou, China, in 1991. He received the B.S. degree in 2015. He is currently a master degree candidate at the Lanzhou University of Technology, Gansu, China, in 2018. His interests include wind energy conversion, microgrids, power system control and distribute generation sources connected to the distribution grid.

Hao Xiaohong, he received the M.S. degree in the control theory and control engineering from Gansu University of Technology, Gansu, China, in 1996. He is now professor, doctoral supervisor at College of Electrical and Information Engineering Lanzhou University of Technology, where he teaches courses on power electronics, control theory. He interests include complex system control, intelligent control

